NeuroImage 225 (2021) 117505

Contents lists available at ScienceDirect

NeuroImage

journal homepage: www.elsevier.com/locate/neuroimage

Characterisation of white matter asymmetries in the healthy human brain using diffusion MRI fixel-based analysis

Arush Honnedevasthana Arun[a,b,d], Alan Connelly[a,b], Robert E. Smith[a,b,1], Fernando Calamante[b,c,d,1,*]

[a] Florey Institute of Neuroscience and Mental Health, Melbourne, Australia
[b] Florey Department of Neuroscience and Mental Health, University of Melbourne, Melbourne, Australia
[c] The University of Sydney, Sydney Imaging, Sydney, Australia
[d] The University of Sydney, School of Biomedical Engineering, Sydney, Australia

ARTICLE INFO

Keywords:
White matter
Asymmetry
Diffusion MRI
Fixel-based analysis

ABSTRACT

The diffusion tensor model for diffusion MRI has been used extensively to study asymmetry in the human brain white matter. However, given the limitations of the tensor model, the nature of any underlying asymmetries remains uncertain, particularly in crossing fibre regions. Here, we provide a more robust characterisation of human brain white matter asymmetries based on fibre-specific diffusion MRI metrics and a whole-brain data-driven approach. We used high-quality diffusion MRI data (n = 100) from the Human Connectome Project, the spherical deconvolution model for fibre orientation distribution estimation, and the Fixel-Based Analysis framework to utilise crossing fibre information in registration, data smoothing and statistical inference. We found many significant asymmetries, widespread throughout the brain white matter, with both left>right and right>left dominances observed in different pathways. No influences of sex, age, or handedness on asymmetry were found. We also report on the relative contributions of microstructural and morphological white matter properties toward the asymmetry findings. Our findings should provide important information to future studies focussing on how these asymmetries are affected by disease, development/ageing, or how they correlate to functional/cognitive measures.

1. Introduction

Despite both hemispheres of the brain sharing broadly the same topographical and surface anatomy, studies have demonstrated the presence of both functional and structural hemispheric asymmetries. In particular, the existence of white matter asymmetry has been confirmed in post-mortem studies in humans (Catani and Budisavljević, 2014; Highley et al., 1999; Toga et al., 2009), including in language-related pathways (Bishop, 2013), cortico-spinal tracts (CST) (Rademacher et al., 2001), uncinate fasciculi, and the optic radiations (Bürgel et al., 1999). However, invasive methods such as blunt dissections and staining of axons have provided only limited information regarding the asymmetry of the relevant fibre bundles (Bürgel et al., 1999). Modern neuroimaging techniques have made it possible to comprehensively characterise asymmetry in terms of structure in vivo. For example, language and auditory processing regions have shown an increase in tract volume in the left hemisphere, based on non-invasive modern imaging methods in healthy subjects (Powell et al., 2006).

In this context, diffusion MRI, and in particular Diffusion Tensor Imaging (DTI), has been used extensively to study white matter structural asymmetry non-invasively. DTI provides a means to analyse the microstructural organisation of white matter fibres in the brain by characterising the anisotropic diffusion of water molecules in each voxel using a symmetric rank-2 tensor (Basser et al., 1994; Catani et al., 2003, 2005). DTI, and diffusion MRI more broadly, can also be used in combination with a fibre-tracking algorithm to reconstruct the white matter pathways in the brain (Tournier et al., 2011), which expands the range of diffusion MRI analysis techniques by which white matter asymmetries may be quantified.

DTI-based methods for assessing white matter asymmetry have been mostly based on measuring volumes of reconstructed tracts and the anisotropy of the tensor model within regions of interest (ROIs) corresponding to white matter structures. For example, DTI studies of white matter asymmetry based on ROI analysis have included evaluation of arcuate fasciculus and language pathways (Catani et al., 2007), the cingulate bundles (Kubicki et al., 2003), the internal capsules

* Correspondence to: The University of Sydney, Brain and Mind Centre, 94 Mallett Street, Camperdown, NSW 2050, Australia.
E-mail address: fernando.calamante@sydney.edu.au (F. Calamante).
[1] These authors have contributed equally.

https://doi.org/10.1016/j.neuroimage.2020.117505
Received 21 February 2020; Received in revised form 18 September 2020; Accepted 22 October 2020
Available online 2 November 2020

(Peled et al., 1998) and the uncinate fasciculi (Kubicki et al., 2002) of healthy subjects. This type of ROI-based approach, however, requires an *a priori* hypothesis to pre-define the region(s) of interest to be assessed.

Alternatively, whole-brain voxel-based strategies can assess areas of structural asymmetry in a more data-driven way. In particular, DTI-based studies have used voxel-based analysis (VBA) in conjunction with fractional anisotropy (FA) maps to identify asymmetries in the arcuate fasciculi, cingulum bundles, and cortico-spinal tracts, amongst others (Büchel et al., 2004; Hidemasa Takao et al., 2011).

Overall, DTI based studies have revealed asymmetry in several white matter regions (see Table 1). However, there are major shortcomings in the DTI model that make asymmetry analyses based on this model unreliable and of limited interpretability. One of the limitations of the diffusion tensor model is that it is not capable of appropriately modelling regions that have complex fibre architecture (such as crossing fibres); this is highly prevalent in the human brain white matter, with evidence that up to 90% of the white matter voxels may contain such fibre configurations (Jeurissen et al., 2013). Accordingly, this makes FA (and other tensor-based metrics) an unreliable measure to assess white matter 'integrity' (Assaf and Pasternak, 2008): a single voxel may be composed of multiple fibre populations with different spatial orientations, therefore a change in FA cannot be easily interpreted given that it is affected by changes in any one of a range of parameters of the individual fibre bundles (e.g. relative orientation, volume fraction, fibre orientation dispersion).

More advanced models for diffusion MRI data, such as spherical deconvolution (Tournier et al., 2004, 2007), can be used to estimate the distribution of fibre orientations (also known as the fibre orientation distribution or FOD) in a voxel, even in the presence of multiple fibre populations. In addition, the FOD amplitude has been suggested as a quantitative measure of the intra-cellular volume of underlying fibre populations, and has been initially termed Apparent Fibre Density (AFD) (Raffelt et al., 2012b). Analysis techniques based on such models therefore provide a means to assess the white matter in a fibre-specific and physically interpretable way.

In this context, Fixel-Based Analysis (FBA) is a recently developed analytical framework that facilitates the evaluation of fibre-specific properties in the white matter from higher-order models such as spherical deconvolution, and hence allows statistical analysis of quantitative measures in the presence of complex fibre geometry in the white matter (Raffelt et al., 2017a, 2017b). Here, the term "fixel" denotes a specific ***fi***bre population within a single vo***xel*** (Raffelt et al., 2015). FBA is capable of separately examining multiple fibre bundle populations within a voxel and enables the evaluation of both microscopic (i.e. intra-axonal fibre volume: "Fibre Density (FD)" Raffelt et al., 2017a, 2017b) and morphological (i.e. changes in macroscopic bundle width: "Fibre Cross-section (FC)" Raffelt et al., 2017a, 2017b) effects in the white matter.

In this work, we used the FBA framework to study asymmetries in the healthy human brain. We aim to provide a more robust characterisation of structural white matter asymmetries than those previously derived using the tensor model, by using quantitative measures derived from the spherical deconvolution model, and a whole-brain data-driven statistical inference framework that is both sensitive and specific to crossing fibres; we furthermore apply this approach to a state-of-the-art publicly available diffusion MRI dataset.[2]

2. Methods

The use of FBA to investigate brain asymmetries necessitated deviations from the example FBA processing pipeline[3] in *MRtrix3* (Tournier et al., 2019). Fig. 1 shows the main steps of our analysis pipeline, with those steps that differ from a typical group comparison FBA experiment highlighted by blue boxes.

2.1. MRI data

We analysed 100 pre-processed Diffusion Weighted Imaging (DWI) datasets from the Human Connectome Project (HCP), aged between 22 and 35 years. The group consisted of 46 males (29.0 ± 3.7 years) and 54 females (29.1 ± 3.6 years). All data were acquired using a modified Siemens 3T scanner ('Connectom Skyra'), whose stronger gradients allow shortening of the diffusion encoding period and decreasing the echo time (TE), thus increasing the signal-to-noise ratio (SNR) (Sotiropoulos et al., 2013). These datasets had 90 gradient directions acquired for each of three b-value shells ($b = 1000$, 2000 and 3000 s/mm^2), with eighteen $b = 0$ s/mm^2 images interspersed, and a spatial resolution of 1.25 mm^3 (Van Essen et al., 2013).

2.2. Image processing

The DWI data provided by HCP were already preprocessed to reduce motion, susceptibility distortions, gradient nonlinearity-induced geometric distortions and eddy current artefacts (Glasser et al., 2013). FODs were calculated using the multi-shell, multi-tissue constrained spherical deconvolution (MSMT-CSD) algorithm (Jeurissen et al., 2014), utilising group averaged response functions for white matter, grey matter and CSF (Dhollander et al., 2016; Raffelt et al., 2012a). FODs were globally normalised to correct for image intensity differences between subjects (Raffelt et al., 2017a, 2017b).

All subject FOD images were used to create a *symmetric* template. To this end, as part of our modified FBA pipeline, a copy of the FOD data from each subject was left/right flipped, and all 200 FOD images (both original and flipped data for all 100 subjects) were used to generate an unbiased symmetric population-specific template (Raffelt et al., 2012a); this step ensures spatial correspondence both between hemispheres and across subjects.

For every voxel within the space of this template image, the template FODs, as well as the non-linearly warped FODs from each input image, were segmented into discrete fixels, each with an associated fibre orientation and density (Smith et al., 2013). Determination of correspondence between the fixels of each input image and those of the template was performed (Raffelt et al., 2017a, 2017b). Because two FOD images were used for each subject (one original and one left-right flipped), for each template fixel, there were *two* values of any fixel-wise metric of interest (one for each hemisphere). In this study, we utilised specifically the "*Fibre Density and Cross-section (FDC)" metric* for statistical analysis. This parameter provides an approximate quantification of the white matter's "ability to relay information" (Raffelt et al., 2017a, 2017b), in that it changes in proportion to both microstructural (in the form of intra-cellular fibre volume: "Fibre Density (FD)" Raffelt et al., 2017a, 2017b) and morphological (i.e. changes in macroscopic bundle width: "Fibre Cross-section (FC)" Raffelt et al., 2017a, 2017b) bundle properties that modulate this capability; it thus acts as an appropriate single scalar measure for statistical inference. Consequences of this decision are discussed further in Section 4.1.

2.3. Statistical analysis

The General Linear Model (GLM) was used to test hypotheses of differences in the *FDC* metric between the left and right hemispheres of the brain (Winkler et al., 2014). This was achieved as part of our modified FBA pipeline as follows: for each subject, we explicitly computed the difference in the value of *FDC* in each fixel between the left and right hemispheres (FDC_R - FDC_L); we performed two independent one-sample t-tests (i.e., $H_{R>L}$: FDC_R - $FDC_L > 0$; $H_{L>R}$: FDC_L - $FDC_R > 0$), with age, sex, and handedness included as covariates (hypotheses of the influence of

[2] A preliminary version of this work was presented at the 27th Annual Meeting of the International Society for Magnetic Resonance in Medicine (ISMRM), Montreal, Canada, 11-16 May 2019, 27: 3618 (2019).

[3] https://mrtrix.readthedocs.io/en/latest/fixel_based_analysis/mt_fibre_density_cross-section.html

Table 1
Summary of findings reported from this study and from prior DTI based asymmetry studies, as well as from the voxel-based FA analysis from the Supplementary Material. Note that the references from prior literature are not meant to represent a comprehensive list; examples listed here are included as a general summary of the overall status of the field. For the prior results reported here, we also considered the arcuate fasciculus to overlap with part of SLF II and SLF IV (Makris et al., 2005). *no overlap in the left and right asymmetry locations.

Structures	Asymmetry from our FBA	α - Relative contribution of FD vs FC	Reports from other studies			Asymmetry from our VBA	
			Asymmetry	Metric	Reference		
Cingulum	LEFT	0.795	LEFT	FA	Gong et al., 2005 Kubicki et al., 2003	LEFT	
				FA, Number of streamlines, Tract volume	Thiebaut de Schotten et al., 2011		
Inferior longitudinal fasciculus	LEFT	0.845	RIGHT	Tract Volume	Latini et al., 2017	LEFT	
				FA	Park et al., 2004		
			LEFT	Tract volume	Panesar et al., 2018		
				FA	Thiebaut de Schotten et al., 2011		
			No Significance	FA	Thomas et al., 2015		
Internal capsule (anterior)	RIGHT	0.601	RIGHT	FA	Park et al., 2004 Peled et al, 1998	LEFT	
Internal capsule (posterior)	LEFT	0.30	RIGHT	FA	Park et al., 2004 Peled et al., 1998	LEFT	
Optic radiations	LEFT	0.665	LEFT	FA	Park et al., 2004 Dayan et al., 2015 Kang et al., 2011	LEFT	
				Post-mortem	Bürgel et al., 1999		
				Volume and shape	Kammen et al., 2016 Chamberland et al., 2018; Dreessen de Gervai et al., 2014; James et al., 2015; Lilja et al., 2014; Yogarajah et al., 2009		
			RIGHT	FA	Thiebaut de Schotten et al., 2011		
Superior longitudinal fasciculus I	LEFT	0.648	LEFT	FA and LA (lattice anisotropy)	Makris et al., 2005	LEFT	
				Number of streamlines, Tract volume	Budisavljevic et al., 2017		
			RIGHT	FA, Number of streamlines	Thiebaut de Schotten et al., 2011 Park et al., 2004		
			No Significance	Tract volume, FA, MD	Kamali et al., 2014		
Superior longitudinal fasciculus II	LEFT	0.72	LEFT	FA and LA (lattice anisotropy)	Makris et al., 2005	LEFT*	RIGHT*
				Streamline end points	Wang et al., 2016		
			No Significance	Tract volume, FA, MD	Kamali et al., 2014		
Superior longitudinal fasciculus IV	RIGHT	0.75	RIGHT	Tract Volume	Thiebaut de Schotten et al., 2011	RIGHT	
				FA	Park et al., 2004		
			LEFT	Volume of streamlines	Fernández-Miranda et al., 2015		
				Relative fibre density	Vernooij et al., 2007		
				FA and LA (lattice anisotropy)	Makris et al., 2005		
Uncinate fasciculus	RIGHT	0.25	RIGHT	Post-mortem	Highley et al., 2002	LEFT	
				Tract volume	Hau et al., 2016		
				FA	Thomas et al., 2015		
			LEFT	FA	Kubicki et al., 2003 Hasan et al., 2009		
				Tract volume and FA correlated with functional task	Ocklenburg et al., 2014		
			No Significance	FA, Number of streamlines	Thiebaut de Schotten et al., 2011		
Inferior fronto-occipital fasciculus	RIGHT	0.70	RIGHT	Tract volume	Hau et al., 2016	RIGHT	
				Number of streamlines	Thiebaut de Schotten et al., 2011		
			LEFT	Tract volume	Hau et al., 2016		
Superior-fronto occipital fasciculus	RIGHT	0.344	No asymmetry-based literature found			LEFT	
Stria terminalis	RIGHT	0.816	No asymmetry-based literature found			LEFT	

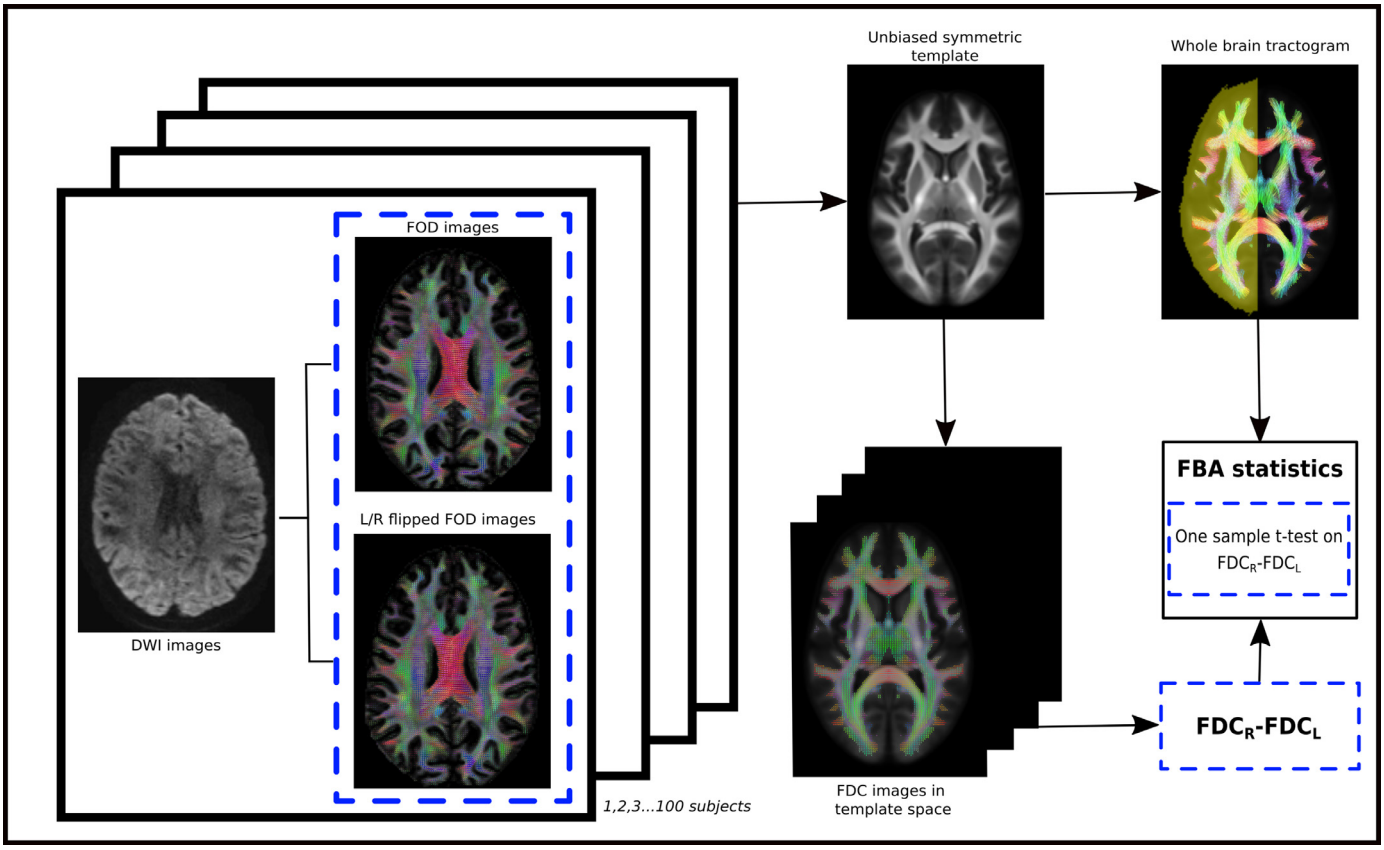

Fig. 1. Flow chart summarising the steps involved in the fixel-based analysis (FBA) for the white matter asymmetry characterisation. The blue dashed box indicates modified part of the traditional FBA pipeline. Pre-processed DWI data were obtained for each of the 100 subjects. Multi-shell, multi-tissue constrained spherical deconvolution (MSMT-CSD) was performed to obtain FOD's and each FOD image was left-right flipped. The flipped and original FOD data were warped to a symmetric template. Fibre-Density cross-section (FDC) was computed for both flipped and original FOD dataset ($n = 200$) by following the standard FBA pipeline. We explicitly computed the difference in the value of FDC in each fixel between the left (L) and right (R) hemispheres (FDC_R - FDC_L). One-sample t-tests were performed to test $FDC_R > FDC_L$ and $FDC_L > FDC_R$ with age, sex, and handedness as covariates. A mask was used to crop the streamlines crossing the mid-sagittal plane and was used to perform data smoothing and statistical enhancement. Family-wise error (FWE) corrected p-values were assigned to each fixel based on 10,000 random shuffles, with statistical significance determined at $p<0.05$. We used a hemisphere mask to test our hypotheses only on the right half of the brain.

these variables on the inter-hemispheric differences were also tested); for statistical inference, all hypotheses were tested in the right hemisphere of the template. To aid visualisation, some results are displayed in the hemisphere of dominance (e.g. Left>Right findings displayed in the left hemisphere) – this is made explicit on each occasion.

The Connectivity-based Fixel Enhancement (CFE) method was used both for tailored smoothing of fixel-wise data, and statistical enhancement of fixel-wise statistical measures (Raffelt et al., 2015). To this end, a whole-brain tractogram of 20 million streamlines was generated using the probabilistic streamlines algorithm iFOD2 (Tournier et al., 2010) on the population FOD template. These data were reduced to a tractogram of 2 million streamlines using the Spherical-deconvolution Informed Filtering of Tractograms (SIFT) algorithm to reduce reconstruction biases (Smith et al., 2013). Streamlines within this tractogram crossing the mid-sagittal plane were cropped in order to prevent data smoothing & statistical enhancement across hemispheres.

Family-wise error (FWE) corrected p-values were assigned to each fixel based on 10,000 random shuffles, with statistical significance determined at $p<0.05$. Our statistical analysis also included a non-parametric non-stationarity correction to compensate for differences in statistical power across the template (Salimi-Khorshidi et al., 2011).

In order to further characterise the observed FDC asymmetries, we evaluated the relative contributions of the fibre density (FD, i.e., microstructure) and fibre cross-section (FC, i.e., morphologic) measures to detected FDC asymmetries (note that FDC is the product of FD and FC Raffelt et al., 2017a, 2017b). To this end, the following steps were carried out:

- Interhemispheric differences ($\Delta = (H_R - H_L)$) and means ($\mu = (H_R + H_L)/2$) were computed from the smoothed fixel data for both FD and FDC metrics.
- For each of FD and FDC independently, the relative change was calculated; i.e., $\mathcal{Q}_{FD} = \Delta_{FD}/\mu_{FD}$ and $\mathcal{Q}_{FDC} = \Delta_{FDC}/\mu_{FDC}$, to compute the relative interhemispheric difference for each metric.
- The ratio of the above 2 measures, i.e. $\alpha = \mathcal{Q}_{FD}/\mathcal{Q}_{FDC}$, was then computed to indicate the relative contribution of FD (and therefore implicitly of FC) to the observed FDC change:
  - $\alpha<0.5$ suggests significant results in FDC are more substantially driven by hemisphere differences in FC, with 0.0 indicating that the observed difference is *entirely* due to a difference in FC;
  - $\alpha>0.5$ suggests results are more greatly driven by hemispheric differences in FD, with 1.0 indicating that the observed difference in FDC is *entirely* due to a difference in FD.

For a set of major white matter regions detected in our study (see Results section), fixel masks corresponding to statistically significant fixels within those regions were used to extract the mean value of this relative contribution parameter per significant bundle.

Note: For completeness, and to allow readers to directly relate some of the prior DTI-based voxel-based results cited in Table 1 to what may have been obtained from the high-quality HCP data used here, we have

included as Supplementary Material ("Voxel-based FA analysis") the results of performing a more traditional voxel-based analysis of FA (in contrast to the fixel-based analysis of the FDC measure, as per the objective of our study). Note however that our study is not intended to perform a head-to-head comparison of these two methods, nor do we attempt to disentangle contributions from the myriad differences in these two analysis pipelines toward their differential results.

2.4. Visualisation

To aid visualisation of the significant results, we isolated from the whole-brain tractogram (which was used for fixel-wise data smoothing and statistical enhancement; see the previous section) only those streamline *segments* for which a statistically significant effect was observed within the underlying fixels traversed.

A track-density imaging (TDI) white matter atlas (Cho et al., 2015) was used to assign anatomical labels to groups of significant fixels. Correspondence of our data with the atlas was achieved by overlaying our significant results on the super-resolution DEC (Directionally-encoded colour) TDI map (Calamante et al., 2010) (generated using the whole-brain tractogram, and computed at 0.5 mm isotropic resolution), oriented such that axial slices were aligned to the central intercommissural line (as was used in the generation of the atlas). Areas contributing to asymmetry were identified by matching the significant fixel results as seen on the slices (axial, coronal and sagittal) of DEC TDI images with the anatomically correspondent slices of the atlas (axial, coronal and sagittal).

Finally, to further visualise the complete trajectories of some of the major white matter bundles where asymmetry was detected, the whole-brain tractogram was edited to isolate those streamlines (in this case the *full* streamlines, not just streamline segments) traversing significant fixels determined to correspond to known anatomical pathways. This visualisation thus allows displaying the full length of these white matter pathways, all the way to the cortical regions to which they are estimated to project.

3. Results

Our statistical analysis identified an extensive breadth of white matter areas demonstrating hemispheric asymmetry in the fixel-specific metric FDC. Fig. 2A and B shows example axial slices of the template image, with significant fixels (FWE-corrected p-value < 0.05) found to have rightward dominance (i.e., $FDC_R > FDC_L$) and leftward dominance (i.e., $FDC_L > FDC_R$) respectively. To aid visualisation, results are shown in the right side of the brain for right>left and in the left side of the brain for the left>right case. For comparison of the relative spatial locations of various white matter bundles for asymmetries observed in either direction, Supplementary Fig. S1 shows streamlines segments associated with significant fixels for both $FDC_R > FDC_L$ and $FDC_L > FDC_R$ results overlaid on the same template image (in this case, with both results displayed on the right hemisphere). Supplementary videos 1 and 2 show animations of the significant results for $FDC_R > FDC_L$ and $FDC_L > FDC_R$ respectively. Statistical tests for the influence of sex, age and handedness on asymmetry revealed no significant effects.

Table 1 lists white matter structures that showed asymmetries and that could be unambiguously identified based on comparison to the white matter atlas, as well as by the complementing information of the trajectories obtained from the white matter bundles isolated from the whole-brain tractogram based on significant fixels (see Section 2.4 Visualisation). Note: as this atlas did not explicitly label the arcuate fasciculus (AF), and to facilitate comparison with prior literature (given AF labelling has been widely adopted in the diffusion MRI field), we consider here that AF overlaps with parts of SLF II and SLF IV (Makris et al., 2005). Reconstructions of complete bundle trajectories for some of the major white matter structures exhibiting asymmetry are shown in Fig. 3. These visualisations were generated only for a subset of the structures identified in Table 1, based on the degree of certainty with which the subset of streamlines traversed the relevant statistically significant fixels, and whose trajectories corresponded to a known white matter bundle.

Fig. 4 illustrates the relative contribution of microstructural (i.e. FD metric) vs. macroscopic (i.e. FC metric) fixel-wise measures to the observed FDC asymmetry effects in white matter regions as listed in Table 1. Supplementary videos 3 and 4 shows an animation of these relative contributions (from FD and FC) to the fixel-wise FDC effect for both right > left and left > right respectively. Table 1 additionally provides the mean of this value within those statistically significant fixels corresponding to each of the identified white matter structures. Values of α for statistically significant pathways were all between 0.0 and 1.0, meaning that none of these pathways demonstrated opposing directionality of asymmetry between the FD and FC metrics.

4. Discussion

The goal of this study was to characterise white matter asymmetries in healthy humans using state-of-the-art diffusion MRI data, a fibre-specific diffusion model metric, and a statistical method that is robust to the presence of complex macroscopic architecture encountered throughout the human brain white matter. We demonstrated the presence of both left-dominated and right-dominated asymmetries in the FDC metric in a large number of white matter structures (as shown in Table 1) using the FBA framework. The findings reported in this study are broadly consistent with those reported by previous DTI and structural studies (Büchel et al., 2004; Catani et al., 2007; Park et al., 2004; Powell et al., 2006; Thiebaut de Schotten et al., 2011); see "Comparison to prior related literature" section below for further discussion. Our study was entirely data-driven: we did not require a prior hypothesis to restrict our analysis to specific white matter regions, instead we tested our hypotheses throughout the entire brain white matter.

As our analysis was based on the FBA framework, it benefits from a number of important strengths of this method in the context of the study of brain asymmetry relative to prior DTI-based literature. These include:

- *Fibre specificity*: Fig. 5 illustrates the most extreme case of the benefits of intra-voxel fibre specificity: voxels may contain fixels for which the direction of the observed effect is reversed (i.e., $FDC_L > FDC_R$ in one fixel and $FDC_R > FDC_L$ in another fixel) *within the same voxel*. Such opposing effects in the fibre bundles within a voxel would potentially be missed by a *voxel*-based analysis approach (as these contributions could have cancelled out in a voxel-aggregate measure). Moreover, the reduced specificity with voxel-based approaches make interpretation of any detectable effect much more complex. A significant result observed with FBA within a template fixel is always specific to that fixel, even in regions containing multiple fibres.
- *Robust template construction*: Previous tensor-based asymmetry studies typically used tensor metrics (Park et al., 2004) (e.g. fractional anisotropy maps) to build a symmetric template. We used FOD-based registration, which is superior to FA-based registration for white matter template construction, as it allows for a better correspondence of white matter anatomical structures across subjects (Raffelt et al., 2012a, 2011), in addition to between hemispheres in this case.
- *Fibre tract-specific smoothing and statistical enhancement*: In FBA, fixel-fixel connectivity information is used to perform smoothing and statistical enhancement in a manner faithful to the fibrous nature of the underlying white matter anatomy; this is preferable to voxel-based techniques, which use only spatial proximity during smoothing, potentially blurring information between adjacent yet unrelated tracts.

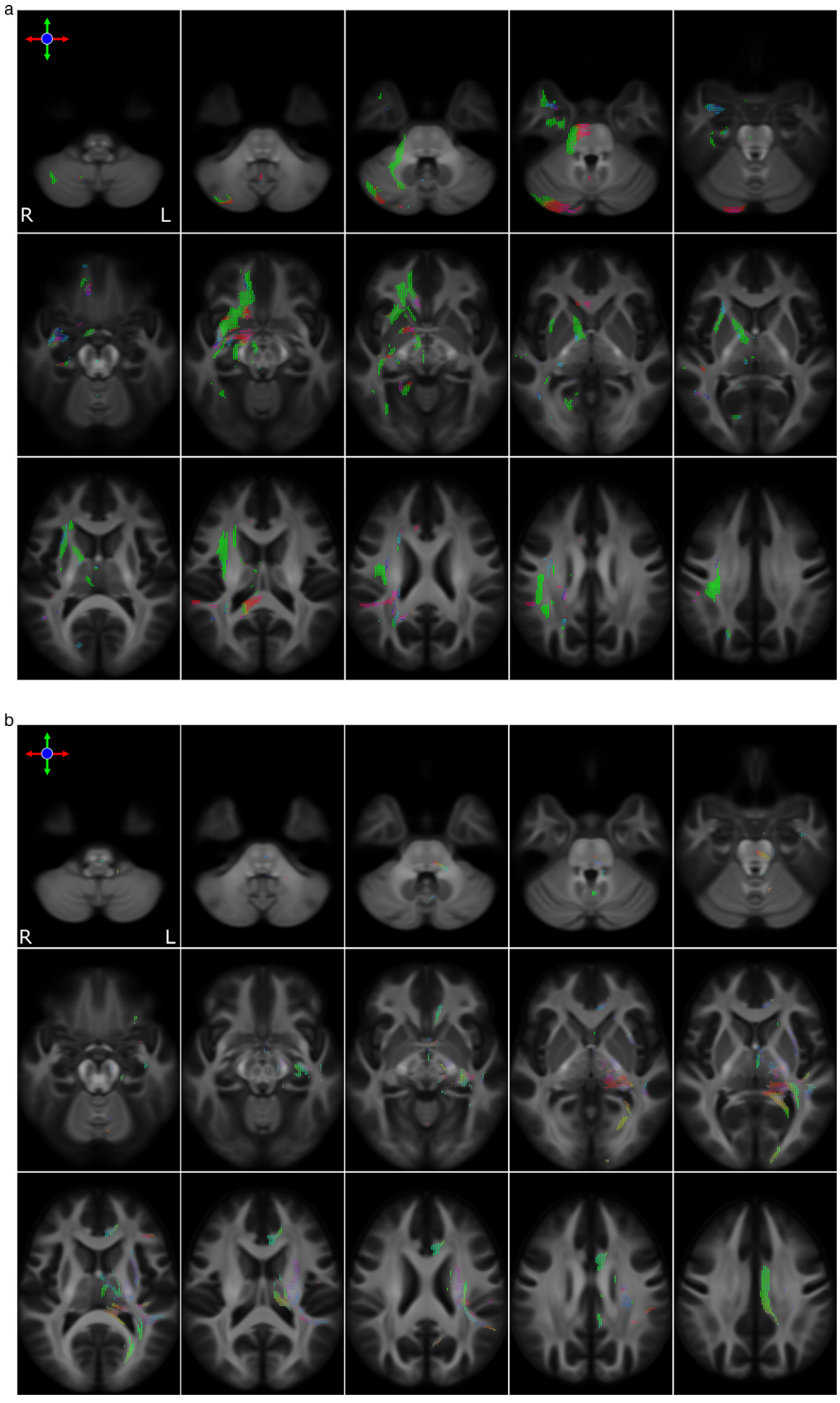

Fig. 2. A- Significant fixels displayed for Right > Left asymmetry (FWE corrected, $p<0.05$) in Fibre Density and Cross-section (FDC). Fixels are displayed in the right hemisphere of the brain as seen on axial slices.
B- Significant fixels displayed for Left>Right asymmetry (FWE corrected, $p<0.05$) in Fibre Density and Cross-section (FDC). Fixels are displayed in the left hemisphere of the brain as seen on axial slices. Fixels coloured according to their fibre orientation (left-right: red; anterior-posterior: green; superior-inferior: blue).

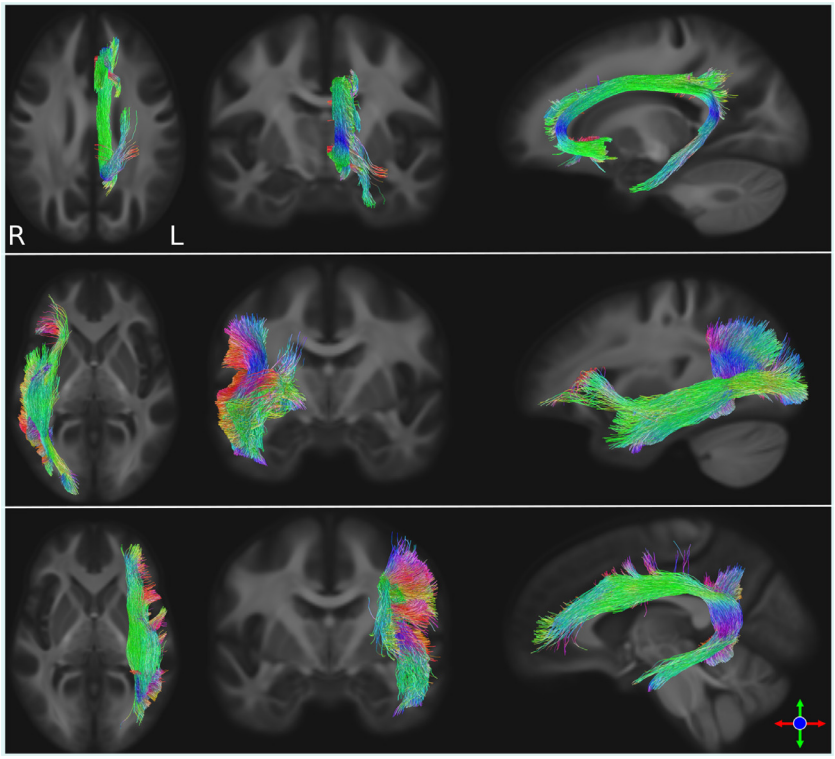

Fig. 3. Visualisation of streamlines traversing significant fixels corresponding to example known anatomical pathways. Top row: left cingulum bundle; middle row: right Inferior Fronto-Occipital Fasciculus; last row: left Superior Longitudinal Fasciculus (note: this bundle also includes part of the arcuate fasciculus, as the latter overlaps with SLF II and SLF IV). Streamlines are coloured according to their local orientation (left-right: red; anterior-posterior: green; superior-inferior: blue). Left: axial view; middle: coronal view; right: sagittal view. Each bundle is shown in the hemisphere in which FDC is greater.

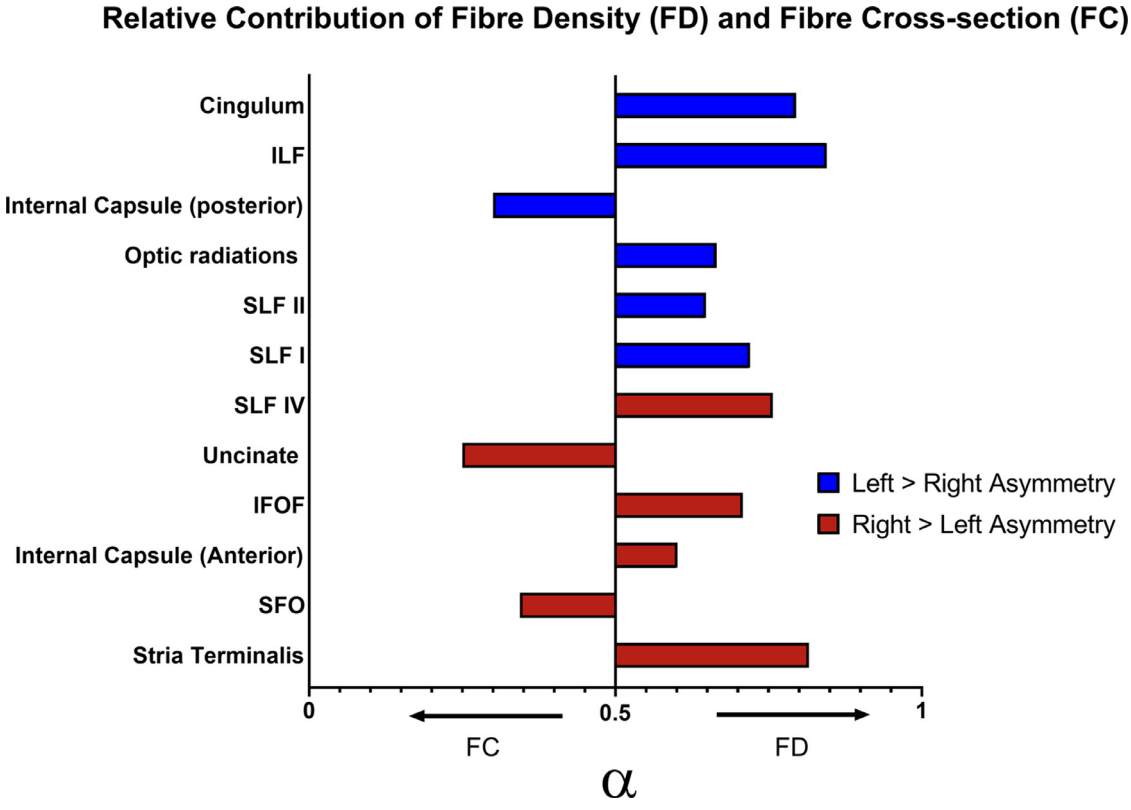

Fig. 4. Relative contribution of FD and FC in the white matter bundles showing significant asymmetry. Parameter α indicates the relative contribution of FD and FC to the observed effect in FDC for each white matter bundle (see Statistical Analysis section). Values less than 0.5 suggest significant results in FDC are primarily driven by hemisphere difference in FC; values greater than 0.5 suggest results are primarily driven by hemispheric differences in FD. ILF: Inferior Longitudinal Fasciculus; SLF: Superior Longitudinal Fasciculus; IFOF: Inferior Fronto-Occipital Fasciculus; SFO: Superior Fronto-Occipital Fasciculus.

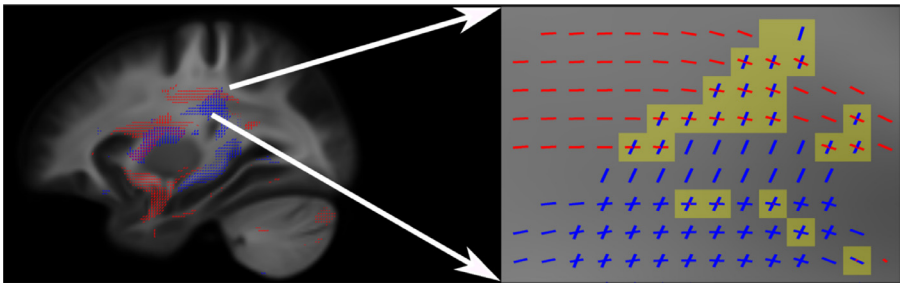

Fig. 5. Example of detected asymmetries (with *R>L* and *L>R* in the same voxel). Red fixels denote *R>L* asymmetry and blue fixels denote *L>R* asymmetry, with both results shown in the right hemisphere to help visualise the relative spatial locations. Yellow voxels indicate overlapping fixels of right/left asymmetry. This demonstrates a strength of FBA, which can characterise asymmetries even in voxels where crossing fibre bundles have opposing asymmetry effects.

4.1. Utilisation of the FDC metric for analysis

While the FBA framework can be applied to assess any number of quantitative diffusion metrics - and all three of the FD, FC and FDC metrics are all tested almost ubiquitously - in this study, we focussed primarily on FDC, for a number of reasons:

- FDC encapsulates both microstructural and morphological changes, and therefore provides an appropriate singular summary measure of the white matter's ability to transfer information - and thus any hemispheric dominance of such in our work – simplifying the interpretation of experimental outcomes.
- This reduces our vulnerability to false positives when testing multiple hypotheses under weak FWE control (Alberton et al., 2020).
- It avoids the potential issue of independent statistical testing of FD and FC despite their potential covariance (Raffelt et al., 2017a, 2017b).
- We interrogated the relative contributions of microstructural and morphological parameters (Fig. 4) to the statistically significant white matter bundle asymmetries by instead estimating the *relative contributions* of these parameters toward the observed FDC effect; this we purport provides comparable information to testing all three conventional FBA metrics, but without necessitating performing explicit statistical inference on each measure individually.

4.2. Comparison to prior related literature

The most commonly used diffusion metrics to measure asymmetry have been FA and tract volume. FA is typically considered to be sensitive to "microstructure" in some way, whereas tract volume is considered to provide an insight into bundle morphology. These physical attributes are comparably interrogated by the FBA metrics FD and FC respectively. However, it is essential to highlight that FBA offers substantial advantages in the fibre bundle specificity of both the quantitative metrics themselves, and the attribution of statistical significance.

Despite these fundamental differences, our fixel-wise results are nevertheless broadly in agreement with previous studies and our own voxel-based FA analysis (e.g., see Table 1 and Supplementary Material); these are discussed in more detail below.

- *Superior Longitudinal Fasciculus (SLF):* We have reported leftward dominant asymmetry in SLF I and SLF II, for both of which the effect is principally driven by FD (Table 1). SLF I findings are in accordance with a previous diffusion-based study based on streamline count following spherical deconvolution-based tractography (Budisavljevic et al., 2017), as well as with our own VBA supplementary results. SLF II findings are in agreement with a DTI-based study (Makris et al., 2005) and another study based on Diffusion Spectrum Imaging (DSI) analysis and fibre tracking on HCP data, reported leftward asymmetry using streamline count as the metric (Wang et al., 2016); however, other findings reported in (Park et al., 2004; Thiebaut de Schotten et al., 2011) contradict this specific result in our study. In another study (Budisavljevic et al., 2017), SLF II was reported to be symmetrically distributed between the left and right hemispheres. Other DTI-based studies did not find any significant asymmetry in SLF I and II components (Kamali et al., 2014). We have reported rightward dominant asymmetry in SLF IV, with the majority of asymmetry contributed by FD (Table 1). This finding is consistent with some previous diffusion-based studies (Park et al., 2004; Thiebaut de Schotten et al., 2011), but inconsistent with others (Fernández-Miranda et al., 2015; Makris et al., 2005; Vernooij et al., 2007); indeed our own VBA supplementary result itself identified both areas with left>right and right>left areas in SLF II. Such inconsistent findings highlight lack of consensus regarding the asymmetry of SLF. It should be also noted that there can be some differences in the way the AF is considered in terms of the SLF. In some studies (Catani and Thiebaut de Schotten, 2008; Martino et al., 2013) the AF is considered as part of the SLF network, with the AF referred to as the 'perisylvian-SLF' or 'SLF IV'. In other studies, the horizontal component of the AF cannot be distinguished from the SLF II, because the two fibre tracts run horizontally and adjacent to each other (Makris et al., 2005). In our study, and for comparison with prior literature, we used the convention that AF overlaps with parts of SLF II and SLF IV (Makris et al., 2005).
- *Cingulum bundle:* We have reported the supracallosal portion of the cingulum bundle to exhibit leftward asymmetry, with the majority of this asymmetry being contributed by FD (Table 1). This is entirely consistent with previous diffusion MRI studies (Gong et al., 2005; Kubicki et al., 2003; Thiebaut de Schotten et al., 2011), and with our own VBA supplementary analysis.
- *Inferior Fronto-Occipital Fasciculus (IFOF):* We have reported IFOF to have rightward asymmetry, with the majority of this asymmetry contributed by FD (Table 1). This finding is consistent with one previous study based on streamline count (Thiebaut de Schotten et al., 2011) and with our own VBA supplementary analysis; however, another study based on measurements of mean tract termination densities reported some components of the IFOF to be leftward dominant (Hau et al., 2016).
- *Uncinate fasciculus (UF):* We have found the uncinate fasciculus to have rightward asymmetry, predominantly contributed by FC (i.e., tract cross-sectional area) (Table 1). This finding is consistent with previous post-mortem dissection (Highley et al., 2002), DTI-based tract volume (Hau et al., 2016) and FA (Thomas et al., 2015). In contrast, our own VBA supplementary analysis and other studies have reported left > right asymmetry in the uncinate using FA as the metric of interest (Hasan et al., 2009; Kubicki et al., 2002). Another study did not find any significant asymmetry in the uncinate (Thiebaut de Schotten et al., 2011). While these latter results contradict our own, this may be due to the limitations of the DTI model and tracking procedures adopted to measure asymmetry. Both IFOF and uncinate fasciculi are crucial for intra-hemispheric transfer of information between the frontal cortex and the occipital, temporal and parietal cortices, and knowing their asymmetries is fundamental for understanding their role in mediating language semantics (Duffau, 2015; Turken and Dronkers, 2011), so resolution of these discrepancies is warranted.

- *Inferior Longitudinal Fasciculus (ILF):* We have reported left>right asymmetry in the ILF, contributed mainly by FD (Table 1). Some previous studies based on FA (Thiebaut de Schotten et al., 2011) and tract volume (Panesar et al., 2018) have reported leftward dominant asymmetry, which was also consistent with our own VBA supplementary analysis; conversely, other FA (Park et al., 2004) and tract volume (Latini et al., 2017) studies have reported rightward asymmetry. Another study using FA metric did not find any significant asymmetry in the ILF (Thomas et al., 2015). These highly conflicted findings mean that there is no current consensus regarding the asymmetry of the ILF in the literature.
- *Optic Radiation:* We have reported leftward asymmetry for the optic radiations, mainly contributed by the FD metric. Investigations into the asymmetry of this structure using FA are conflicted, with both rightward dominance (Thiebaut de Schotten et al., 2011) and leftward dominance (Dayan et al., 2015; Kang et al., 2011; Park et al., 2004) previously reported. Conflicting reports in FA-based studies may be due to the difference in DTI metrics used to report asymmetry findings. Leftward lateralisation has been reported with respect to volume (Kammen et al., 2016) and shape (larger anterior extent, i.e., smaller optical radiation temporal pole distance (Chamberland et al., 2018; Dreessen de Gervai et al., 2014; James et al., 2015; Lilja et al., 2014; Yogarajah et al., 2009)). Histological studies have reported leftward asymmetry in optic radiation (Bürgel et al., 1999), concordant with the findings reported in our study. Our own VBA supplementary analysis also showed leftward FA asymmetry.
- *Internal Capsule:* For the internal capsule, we found leftward asymmetry (dominated by the contribution of FC) in the posterior aspect and rightward asymmetry (dominated by the contribution of FD) in the anterior part. A previous study based on FA metric reported rightward asymmetry effects for the posterior part of the internal capsule (Park et al., 2004); our own VBA supplementary analysis found leftward asymmetry in both anterior and posterior aspects. This conflict may be due to the presence of crossing fibres at the medial regions where the SLF and fibres from the posterior limb of the internal capsule cross, where DTI-based metrics may yield misleading findings (Tournier et al., 2011).
- Additionally to the above findings, but to the best of our knowledge not reported in any prior diffusion-based asymmetry studies, we found rightward asymmetry in the stria terminalis and SFOF, and leftward asymmetry the in forceps major and corona radiata superior. For comparison, our VBA supplementary analysis showed leftward FA asymmetry in stria terminalis, SFOF, forceps major and corona radiata superior; the conflicting results could again originate in limitations of the tensor model.

We did not find any association of sex, age or handedness with asymmetry in our analysis. This may be, in part, due to the limited age range of our data set (22–35 years) and to the large proportion of right-handed subjects (86%). Literature on the effect of sex, age, and handedness in hemispheric differences is not conclusive. One study with a very large sample size ($n = 857$) reported small regions showing significant effects of age and sex on white matter asymmetry (Takao et al., 2011). In another study investigating the UF with a wide participant age range (6–68), a left > right asymmetry was reported in childhood but conversely a right > left asymmetry in adulthood (Hasan et al., 2010); they did not, however, find significant differences in asymmetry of this bundle between males and females. Similarly, no sex-related differences were reported by a study investigating asymmetry in IFOF (Wu et al., 2016). Another study reported a significant effect of handedness on asymmetry in the frontal lobe using the FA metric (Büchel et al., 2004); however, consistent with our own findings, previous VBM (Good et al., 2001) and DTI (Hervé et al., 2006; Westerhausen et al., 2007) studies failed to demonstrate any asymmetry related to participant handedness. Further research would be necessary to resolve these conflicts in characterisation of the influences of sex, age, and handedness on white matter asymmetry.

In general, it should be noted that findings from asymmetry studies involving DTI (Büchel et al., 2004; Hau et al., 2016; Park et al., 2004; Thiebaut de Schotten et al., 2011; Vernooij et al., 2007) - which is the most widely used strategy - can be challenging to interpret. Not only are such metrics quantified at the voxel level, and therefore cannot be easily attributed to specific fibre bundles, their sensitivity to differential effects within individual crossing fibre bundles is complex and difficult to predict; indeed, in some cases, genuine effects within multiple crossing fibre bundles in a voxel may result in no net observable change in these metrics. The limitations of the tensor model do not only affect voxel-wise quantitative measures, but also the outcomes of tractography, where the inability to properly model the complexity of the underlying fibrous structure can lead to erroneous quantification of features such as tract volume (Farquharson et al., 2013).

4.3. Practical issues and limitations

This study has a number of limitations, which we summarise here:

- We restricted specifically our anatomical labelling of the structures identified as having significant results to only those white matter structures that could be confidently identified based on the TDI human brain atlas (Cho et al., 2015) or also based on the complementary information from fibre-tracking reconstructions based on significant fixels. The set of fixels exhibiting statistical significance is greater than the list of structures in Table 1; the complete uncurated results are shown in Fig. 2A and B, and supplementary videos 1 and 2.
- Fig. 3 shows only a few white matter bundles that could be unambiguously delineated from the whole-brain tractogram based on a cluster of significant fixels. Other white matter bundles identified as statistically significant could not be reconstructed in this manner without considerable manual editing of the tractogram to isolate only those streamlines deemed to correspond to the expected anatomical pathways, which may have subjectively influenced the interpretation of such results. It should be noted, however, that this limitation only influences the labelling / visualisation / reporting aspects of the study, not the statistical inference itself.
- As we sought to maximise our sensitivity to detect a genuine effect, we used in this study data from HCP, as this is amongst the best quality publicly available diffusion MRI data. It was not the purpose of this study to investigate the structures that can still be reliably identified as asymmetric using more typical clinical diffusion MRI protocols. Further work is also needed to fully characterise how the various protocol parameters impact the findings from FBA. While some parameters have been explored elsewhere (e.g. *b*-value dependency (Genc et al., 2020; Raffelt et al., 2012b), more thorough evaluation of the sensitivity of FBA to experimental conditions would provide useful information.
- We observed asymmetry in a small number of interhemispheric white matter connections, in both our primary FBA of FDC and our supplementary VBA of FA. This was an unexpected finding, as one would intuitively expect that the white matter properties reflected by the FDC metric should not vary on either side of the interhemispheric plane. It has not yet been ascertained whether this effect is due to asymmetry of the gradient non-linearities of the Connectom Skyra hardware or inter-hemispheric differences in tissue magnetisation properties such as T_2 (neither of which can currently be handled appropriately within the spherical deconvolution model used), some other aspect of our processing pipeline, or a genuine biological difference.
- As discussed in the previous section, there were a number of structures for which our findings disagreed with those from some published data. This is not novel in this context, as there are also in-

consistencies between the asymmetry trends reported amongst prior studies (e.g. see Table 1). While we speculate that the differences between our results and others are likely due to known limitations of the DTI model and analysis methods utilised in prior studies, we cannot definitively assert that our FBA results reflect biological truth and that any disagreement with such must be erroneous, as FBA itself is prone to its own unique set of limitations and artifacts. We do however suggest that the demonstrable technical advantages afforded by utilisation of the FBA framework give greater confidence to the asymmetry results observed using such.

5. Conclusion

We have provided a robust characterisation of white matter asymmetry in the healthy population, using a fibre-specific diffusion metric and analysis framework and high-quality diffusion MRI data. We observed many significant asymmetries, widespread throughout the brain, with both left>right and right>left dominances observed in different pathways. We additionally reported on the relative contributions of microstructural (i.e. Fibre Density) and morphological (i.e. Fibre Cross-section) white matter properties toward these observations. These findings should provide important information to future studies focussing on how these asymmetries are affected by the disease, how asymmetry changes during development/ageing, or how such asymmetries are correlated to functional studies or cognitive measures.

Declaration of Competing Interest

The authors have no conflict of interest to declare.

Acknowledgement

This work was supported by funding from the National Health and Medical Research Council of Australia (grant numbers APP1091593 and APP1117724), the Australian Research Council (grant number DP170101815), the Victorian Government's Operational Infrastructure Support Program, and the Melbourne Bioinformatics at the University of Melbourne, grant number UOM0048. RS is supported by fellowship funding from the National Imaging Facility (NIF), an Australian Government National Collaborative Research Infrastructure Strategy (NCRIS) capability. Data were provided by the Human Connectome Project, WU-Minn Consortium (Principal Investigators: David Van Essen and Kamil Ugurbil; 1U54MH091657) funded by the 16 NIH Institutes and Centers that support the NIH Blueprint for Neuroscience Research; and by the McDonnell centre for Systems Neuroscience at Washington University. The authors acknowledge the technical assistance provided by the Sydney Informatics Hub, a Core Research Facility of the University of Sydney.

Supplementary materials

Supplementary material associated with this article can be found, in the online version, at doi:10.1016/j.neuroimage.2020.117505.

References

Alberton, B.A.V., Nichols, T.E., Gamba, H.R., Winkler, A.M., 2020. Multiple testing correction over contrasts for brain imaging. Neuroimage 216, 116760. doi:10.1016/j.neuroimage.2020.116760.

Assaf, Y., Pasternak, O., 2008. Diffusion tensor imaging (DTI)-based white matter mapping in brain research: a review. J. Mol. Neurosci. 34, 51–61. doi:10.1007/s12031-007-0029-0.

Basser, P.J., Mattiello, J., LeBihan, D., 1994. MR diffusion tensor spectroscopy and imaging. Biophys. J. 66, 259–267. doi:10.1016/S0006-3495(94)80775-1.

Bishop, D.V.M., 2013. Cerebral asymmetry and language development: cause, correlate or consequence? Science 340, 1230531. doi:10.1126/science.1230531.

Büchel, C., Raedler, T., Sommer, M., Sach, M., Weiller, C., Koch, M.A., 2004. White matter asymmetry in the human brain: a diffusion tensor MRI study. Cereb. Cortex 14, 945–951. doi:10.1093/cercor/bhh055.

Budisavljevic, S., Dell'Acqua, F., Zanatto, D., Begliomini, C., Miotto, D., Motta, R., Castiello, U., 2017. Asymmetry and structure of the fronto-parietal networks underlie visuomotor processing in humans. Cereb. Cortex 27, 1532–1544. doi:10.1093/cercor/bhv348.

Bürgel, U., Schormann, T., Schleicher, A., Zilles, K., 1999. Mapping of histologically identified long fiber tracts in human cerebral hemispheres to the MRI volume of a reference brain: position and spatial variability of the optic radiation. Neuroimage 10, 489–499. doi:10.1006/nimg.1999.0497.

Calamante, F., Tournier, J.-.D., Jackson, G.D., Connelly, A., 2010. Track-density imaging (TDI): super-resolution white matter imaging using whole-brain track-density mapping. Neuroimage 53, 1233–1243. doi:10.1016/j.neuroimage.2010.07.024.

Catani, M., Allin, M.P.G., Husain, M., Pugliese, L., Mesulam, M.M., Murray, R.M., Jones, D.K., 2007. Symmetries in human brain language pathways correlate with verbal recall. Proc. Natl. Acad. Sci. USA 104, 17163–17168. doi:10.1073/pnas.0702116104.

Catani, M., Budisavljević, S., 2014. Chapter 22 – contribution of diffusion tractography to the anatomy of language. In: Johansen-Berg, H., Behrens, T.E.J. (Eds.), Diffusion MRI. Academic Press, San Diego, pp. 511–529. doi:10.1016/B978-0-12-396460-1.00022-6.

Catani, M., Jones, D.K., Donato, R., Ffytche, D.H., 2003. Occipito-temporal connections in the human brain. Brain J. Neurol. 126, 2093–2107. doi:10.1093/brain/awg203.

Catani, M., Jones, D.K., ffytche, D.H., 2005. Perisylvian language networks of the human brain. Ann. Neurol. 57, 8–16. doi:10.1002/ana.20319.

Catani, M., Thiebaut de Schotten, M., 2008. A diffusion tensor imaging tractography atlas for virtual in vivo dissections. Cortex 44, 1105–1132. doi:10.1016/j.cortex.2008.05.004, Special issue on "brain hodology – revisiting disconnection approaches to disorders of cognitive function".

Chamberland, M., Tax, C.M.W., Jones, D.K., 2018. Meyer's loop tractography for image-guided surgery depends on imaging protocol and hardware. NeuroImage Clin. 20, 458–465. doi:10.1016/j.nicl.2018.08.021.

Cho, Z.-H., Chi, J.-G., Calamante, F. (Eds.), 2015. 7.0 Tesla MRI Brain White Matter Atlas, 2nd ed.. Springer-Verlag, Berlin Heidelberg.

Dayan, M., Munoz, M., Jentschke, S., Chadwick, M.J., Cooper, J.M., Riney, K., Vargha-Khadem, F., Clark, C.A., 2015. Optic radiation structure and anatomy in the normally developing brain determined using diffusion MRI and tractography. Brain Struct. Funct. 220, 291–306. doi:10.1007/s00429-013-0655-y.

Dhollander, T., Raffelt, D., Connelly, A., 2016. Unsupervised 3-tissue response function estimation from single-shell or multi-shell diffusion MR data without a co-registered T1 image. In: Proceedings of ISMRM Workshop on Breaking the Barriers of Diffusion MRI. Lisbon, Portugal, p. 5.

Dreessen de Gervai, P., Sboto-Frankenstein, U.N., Bolster, R.Bruce., Thind, S., Gruwel, M.L.H., Smith, S.D., Tomanek, B., 2014. Tractography of Meyer's Loop asymmetries. Epilepsy Res. 108, 872–882. doi:10.1016/j.eplepsyres.2014.03.006.

Duffau, H., 2015. Stimulation mapping of white matter tracts to study brain functional connectivity. Nat. Rev. Neurol. 11, 255–265. doi:10.1038/nrneurol.2015.51.

Farquharson, S., Tournier, J.-.D., Calamante, F., Fabinyi, G., Schneider-Kolsky, M., Jackson, G.D., Connelly, A., 2013. White matter fiber tractography: why we need to move beyond DTI. J. Neurosurg. 118, 1367–1377. doi:10.3171/2013.2.JNS121294.

Fernández-Miranda, J.C., Wang, Y., Pathak, S., Stefaneau, L., Verstynen, T., Yeh, F.-.C., 2015. Asymmetry, connectivity, and segmentation of the arcuate fascicle in the human brain. Brain Struct. Funct. 220, 1665–1680. doi:10.1007/s00429-014-0751-7.

Genc, S., Tax, C.M.W., Raven, E.P., Chamberland, M., Parker, G.D., Jones, D.K., 2020. Impact of b-value on estimates of apparent fibre density. Hum. Brain Mapp. 41, 2583–2595. doi:10.1002/hbm.24964.

Glasser, M.F., Sotiropoulos, S.N., Wilson, J.A., Coalson, T.S., Fischl, B., Andersson, J.L., Xu, J., Jbabdi, S., Webster, M., Polimeni, J.R., Van Essen, D.C., Jenkinson, M., Consortium, WU-Minn HCP, 2013. The minimal preprocessing pipelines for the human connectome project. Neuroimage 80, 105–124. doi:10.1016/j.neuroimage.2013.04.127.

Gong, G., Jiang, T., Zhu, C., Zang, Y., Wang, F., Xie, S., Xiao, J., Guo, X., 2005. Asymmetry analysis of cingulum based on scale-invariant parameterization by diffusion tensor imaging. Hum. Brain Mapp. 24, 92–98. doi:10.1002/hbm.20072.

Good, C.D., Johnsrude, I., Ashburner, J., Henson, R.N., Friston, K.J., Frackowiak, R.S., 2001. Cerebral asymmetry and the effects of sex and handedness on brain structure: a voxel-based morphometric analysis of 465 normal adult human brains. Neuroimage 14, 685–700. doi:10.1006/nimg.2001.0857.

Hasan, K.M., Iftikhar, A., Kamali, A., Kramer, L.A., Ashtari, M., Cirino, P.T., Papanicolaou, A.C., Fletcher, J.M., Ewing-Cobbs, L., 2009. Development and aging of the healthy human brain uncinate fasciculus across the lifespan using diffusion tensor tractography. Brain Res. 1276, 67–76. doi:10.1016/j.brainres.2009.04.025.

Hasan, K.M., Kamali, A., Abid, H., Kramer, L.A., Fletcher, J.M., Ewing-Cobbs, L., 2010. Quantification of the spatiotemporal microstructural organization of the human brain association, projection and commissural pathways across the lifespan using diffusion tensor tractography. Brain Struct. Funct. 214, 361–373. doi:10.1007/s00429-009-0238-0.

Hau, J., Sarubbo, S., Perchey, G., Crivello, F., Zago, L., Mellet, E., Jobard, G., Joliot, M., Mazoyer, B.M., Tzourio-Mazoyer, N., Petit, L., 2016. Cortical terminations of the inferior fronto-occipital and uncinate fasciculi: anatomical stem-based virtual dissection. Front. Neuroanat. 10. doi:10.3389/fnana.2016.00058.

Hervé, P.-.Y., Crivello, F., Perchey, G., Mazoyer, B., Tzourio-Mazoyer, N., 2006. Handedness and cerebral anatomical asymmetries in young adult males. Neuroimage 29, 1066–1079. doi:10.1016/j.neuroimage.2005.08.031.

Highley, J.R., McDonald, B., Walker, M.A., Esiri, M.M., Crow, T.J., 1999. Schizophrenia and temporal lobe asymmetry. A post-mortem stereological study of tissue volume. Br. J. Psychiatry J. Ment. Sci. 175, 127–134.

Highley, J.R., Walker, M.A., Esiri, M.M., Crow, T.J., Harrison, P.J., 2002. Asymmetry of the uncinate fasciculus: a post-mortem study of normal subjects and patients with schizophrenia. Cereb. Cortex 12, 1218–1224. doi:10.1093/cercor/12.11.1218.

James, J.S., Radhakrishnan, A., Thomas, B., Madhusoodanan, M., Kesavadas, C., Abraham, M., Menon, R., Rathore, C., Vilanilam, G., 2015. Diffusion tensor imaging tractography of Meyer's loop in planning resective surgery for drug-resistant temporal lobe epilepsy. Epilepsy Res. 110, 95–104. doi:10.1016/j.eplepsyres.2014.11.020.

Jeurissen, B., Leemans, A., Tournier, J.-.D., Jones, D.K., Sijbers, J., 2013. Investigating the prevalence of complex fiber configurations in white matter tissue with diffusion magnetic resonance imaging. Hum. Brain Mapp. 34, 2747–2766. doi:10.1002/hbm.22099.

Jeurissen, B., Tournier, J.-.D., Dhollander, T., Connelly, A., Sijbers, J., 2014. Multi-tissue constrained spherical deconvolution for improved analysis of multi-shell diffusion MRI data. Neuroimage 103, 411–426. doi:10.1016/j.neuroimage.2014.07.061.

Kamali, A., Flanders, A.E., Brody, J., Hunter, J.V., Hasan, K.M., 2014. Tracing superior longitudinal fasciculus connectivity in the human brain using high resolution diffusion tensor tractography. Brain Struct. Funct. 219. doi:10.1007/s00429-012-0498-y.

Kammen, A., Law, M., Tjan, B.S., Toga, A.W., Shi, Y., 2016. Automated retinofugal visual pathway reconstruction with multi-shell HARDI and FOD-based analysis. Neuroimage 125, 767–779. doi:10.1016/j.neuroimage.2015.11.005.

Kang, X., Herron, T.J., Woods, D.L., 2011. Regional variation, hemispheric asymmetries and gender differences in pericortical white matter. Neuroimage 56, 2011–2023. doi:10.1016/j.neuroimage.2011.03.016.

Kubicki, M., Westin, C.-.F., Maier, S.E., Frumin, M., Nestor, P.G., Salisbury, D.F., Kikinis, R., Jolesz, F.A., McCarley, R.W., Shenton, M.E., 2002. Uncinate fasciculus findings in schizophrenia: a magnetic resonance diffusion tensor imaging study. Am. J. Psychiatry 159, 813–820. doi:10.1176/appi.ajp.159.5.813.

Kubicki, M., Westin, C.-.F., Nestor, P.G., Wible, C.G., Frumin, M., Maier, S.E., Kikinis, R., Jolesz, F.A., McCarley, R.W., Shenton, M.E., 2003. Cingulate Fasciculus integrity disruption in schizophrenia: a magnetic resonance diffusion tensor imaging study. Biol. Psychiatry 54, 1171–1180.

Latini, F., Mårtensson, J., Larsson, E.-.M., Fredrikson, M., Åhs, F., Hjortberg, M., Aldskogius, H., Ryttlefors, M., 2017. Segmentation of the inferior longitudinal fasciculus in the human brain: a white matter dissection and diffusion tensor tractography study. Brain Res. 1675, 102–115. doi:10.1016/j.brainres.2017.09.005.

Lilja, Y., Ljungberg, M., Starck, G., Malmgren, K., Rydenhag, B., Nilsson, D.T., 2014. Visualizing Meyer's loop: a comparison of deterministic and probabilistic tractography. Epilepsy Res. 108, 481–490. doi:10.1016/j.eplepsyres.2014.01.017.

Makris, N., Kennedy, D.N., McInerney, S., Sorensen, A.G., Wang, R., Caviness, V.S., Pandya, D.N., 2005. Segmentation of subcomponents within the superior longitudinal fascicle in humans: a quantitative, in vivo, DT-MRI study. Cereb. Cortex 15, 854–869. doi:10.1093/cercor/bhh186.

Martino, J., De Witt Hamer, P.C., Berger, M.S., Lawton, M.T., Arnold, C.M., de Lucas, E.M., Duffau, H., 2013. Analysis of the subcomponents and cortical terminations of the perisylvian superior longitudinal fasciculus: a fiber dissection and DTI tractography study. Brain Struct. Funct. 218, 105–121. doi:10.1007/s00429-012-0386-5.

Ocklenburg S., Schlaffke L., Hugdahl K., Westerhausen R. From structure to function in the lateralized brain: how structural properties of the arcuate and uncinate fasciculus are associated with dichotic listening performance. Neurosci Lett. 2014 Sep 19;580:32-6. doi:10.1016/j.neulet.2014.07.044. Epub 2014 Aug 2.

Panesar, S.S., Yeh, F.-.C., Jacquesson, T., Hula, W., Fernandez-Miranda, J.C., 2018. A quantitative tractography study into the connectivity, segmentation and laterality of the human inferior longitudinal fasciculus. Front. Neuroanat. 12. doi:10.3389/fnana.2018.00047.

Park, H.-.J., Westin, C.-.F., Kubicki, M., Maier, S.E., Niznikiewicz, M., Baer, A., Frumin, M., Kikinis, R., Jolesz, F.A., McCarley, R.W., Shenton, M.E., 2004. White matter hemisphere asymmetries in healthy subjects and in schizophrenia: a diffusion tensor MRI study. Neuroimage 23, 213–223. doi:10.1016/j.neuroimage.2004.04.036.

Peled, S., Gudbjartsson, H., Westin, C.F., Kikinis, R., Jolesz, F.A., 1998. Magnetic resonance imaging shows orientation and asymmetry of white matter fiber tracts. Brain Res. 780, 27–33.

Powell, H.W.R., Parker, G.J.M., Alexander, D.C., Symms, M.R., Boulby, P.A., Wheeler-Kingshott, C.A.M., Barker, G.J., Noppeney, U., Koepp, M.J., Duncan, J.S., 2006. Hemispheric asymmetries in language-related pathways: a combined functional MRI and tractography study. Neuroimage 32, 388–399. doi:10.1016/j.neuroimage.2006.03.011.

Rademacher, J., Bürgel, U., Geyer, S., Schormann, T., Schleicher, A., Freund, H.J., Zilles, K., 2001. Variability and asymmetry in the human precentral motor system. A cytoarchitectonic and myeloarchitectonic brain mapping study. Brain J. Neurol. 124, 2232–2258.

Raffelt, D., Tournier, J.-.D., Crozier, S., Connelly, A., Salvado, O., 2012a. Reorientation of fiber orientation distributions using apodized point spread functions. Magn. Reson. Med. 67, 844–855. doi:10.1002/mrm.23058.

Raffelt, D., Tournier, J.-.D., Fripp, J., Crozier, S., Connelly, A., Salvado, O., 2011. Symmetric diffeomorphic registration of fibre orientation distributions. Neuroimage 56, 1171–1180. doi:10.1016/j.neuroimage.2011.02.014.

Raffelt, D., Tournier, J.-.D., Rose, S., Ridgway, G.R., Henderson, R., Crozier, S., Salvado, O., Connelly, A., 2012b. Apparent fibre density: a novel measure for the analysis of diffusion-weighted magnetic resonance images. Neuroimage 59, 3976–3994. doi:10.1016/j.neuroimage.2011.10.045.

Raffelt, D., Tournier, J.-.D., Smith, R.E., Vaughan, D.N., Jackson, G., Ridgway, G.R., Connelly, A., 2017a. Investigating white matter fibre density and morphology using fixel-based analysis. Neuroimage 144, 58–73. doi:10.1016/j.neuroimage.2016.09.029.

Raffelt, D.A., Smith, R.E., Ridgway, G.R., Tournier, J.-.D., Vaughan, D.N., Rose, S., Henderson, R., Connelly, A., 2015. Connectivity-based fixel enhancement: whole-brain statistical analysis of diffusion MRI measures in the presence of crossing fibres. Neuroimage 117, 40–55. doi:10.1016/j.neuroimage.2015.05.039.

Raffelt, D., Dhollander, T., Tournier, J.-.D., Tabbara, R., Smith, R.E, Pierre, E., Connelly, A., 2017b. Bias field correction and intensity normalisation for quantitative analysis of apparent fibre density. In: Proceedings of the 26th Annual Meeting International Society of Magnetic Resonance in Medicine, ISMRM, 3541. Honolulu, USA.

Salimi-Khorshidi, G., Smith, S.M., Nichols, T.E., 2011. Adjusting the effect of non-stationarity in cluster-based and TFCE inference. Neuroimage 54, 2006–2019. doi:10.1016/j.neuroimage.2010.09.088.

Smith, R.E., Tournier, J.-.D., Calamante, F., Connelly, A., 2013. SIFT: spherical-deconvolution informed filtering of tractograms. Neuroimage 67, 298–312. doi:10.1016/j.neuroimage.2012.11.049.

Sotiropoulos, S.N., Jbabdi, S., Xu, J., Andersson, J.L., Moeller, S., Auerbach, E.J., Glasser, M.F., Hernandez, M., Sapiro, G., Jenkinson, M., Feinberg, D.A., Yacoub, E., Lenglet, C., Van Essen, D.C., Ugurbil, K., Behrens, T.E.J., WU-Minn HCP Consortium, 2013. Advances in diffusion MRI acquisition and processing in the human connectome project. Neuroimage 80, 125–143. doi:10.1016/j.neuroimage.2013.05.057.

Takao, Hidemasa, Abe, O., Yamasue, H., Aoki, S., Sasaki, H., Kasai, K., Yoshioka, N., Ohtomo, K., 2011a. Gray and white matter asymmetries in healthy individuals aged 21-29 years: a voxel-based morphometry and diffusion tensor imaging study. Hum. Brain Mapp. 32, 1762–1773. doi:10.1002/hbm.21145.

Takao, H., Hayashi, N., Ohtomo, K., 2011b. White matter asymmetry in healthy individuals: a diffusion tensor imaging study using tract-based spatial statistics. Neuroscience 193, 291–299. doi:10.1016/j.neuroscience.2011.07.041.

Thiebaut de Schotten, M., Ffytche, D.H., Bizzi, A., Dell'Acqua, F., Allin, M., Walshe, M., Murray, R., Williams, S.C., Murphy, D.G.M., Catani, M., 2011. Atlasing location, asymmetry and inter-subject variability of white matter tracts in the human brain with MR diffusion tractography. Neuroimage 54, 49–59. doi:10.1016/j.neuroimage.2010.07.055.

Thomas, C., Avram, A., Pierpaoli, C., Baker, C., 2015. Diffusion MRI properties of the human uncinate fasciculus correlate with the ability to learn visual associations. Cortex 72, 65–78. doi:10.1016/j.cortex.2015.01.023, The whole is greater than the sum of the parts.

Toga, A.W., Narr, K.L., Thompson, P.M., Luders, E., 2009. Brain asymmetry: evolution. In: Squire, L.R. (Ed.), Encyclopedia of Neuroscience. Academic Press, Oxford, pp. 303–311. doi:10.1016/B978-008045046-9.00936-0.

Tournier, J.-.D., Calamante, F., Connelly, A., 2010. Improved probabilistic streamlines tractography by 2nd order integration over fibre orientation distributions. In: Proceedings of the 18th Annual Meeting International Society of Magnetic Resonance in Medicine, ISMRM, 1670. Stockholm, Sweden, p. 18.

Tournier, J.-.D., Calamante, F., Connelly, A., 2007. Robust determination of the fibre orientation distribution in diffusion MRI: non-negativity constrained super-resolved spherical deconvolution. Neuroimage 35, 1459–1472. doi:10.1016/j.neuroimage.2007.02.016.

Tournier, J.-.D., Calamante, F., Gadian, D.G., Connelly, A., 2004. Direct estimation of the fiber orientation density function from diffusion-weighted MRI data using spherical deconvolution. Neuroimage 23, 1176–1185. doi:10.1016/j.neuroimage.2004.07.037.

Tournier, J.-.D., Mori, S., Leemans, A., 2011. Diffusion tensor imaging and beyond. Magn. Reson. Med. 65, 1532–1556. doi:10.1002/mrm.22924.

Tournier, J.-.D., Smith, R., Raffelt, D., Tabbara, R., Dhollander, T., Pietsch, M., Christiaens, D., Jeurissen, B., Yeh, C.-.H., Connelly, A., 2019. MRtrix3: a fast, flexible and open software framework for medical image processing and visualisation. Neuroimage 202, 116137. doi:10.1016/j.neuroimage.2019.116137.

Turken, A.U., Dronkers, N.F., 2011. The neural architecture of the language comprehension network: converging evidence from lesion and connectivity analyses. Front. Syst. Neurosci. 5. doi:10.3389/fnsys.2011.00001.

Van Essen, D.C., Smith, S.M., Barch, D.M., Behrens, T.E.J., Yacoub, E., Ugurbil, K., 2013. The WU-minn human connectome project: an overview. Neuroimage 80, 62–79. doi:10.1016/j.neuroimage.2013.05.041.

Vernooij, M.W., Smits, M., Wielopolski, P.A., Houston, G.C., Krestin, G.P., van der Lugt, A., 2007. Fiber density asymmetry of the arcuate fasciculus in relation to functional hemispheric language lateralization in both right- and left-handed healthy subjects: a combined fMRI and DTI study. Neuroimage 35, 1064–1076. doi:10.1016/j.neuroimage.2006.12.041.

Wang, X., Pathak, S., Stefaneanu, L., Yeh, F.-.C., Li, S., Fernandez-Miranda, J.C., 2016. Subcomponents and connectivity of the superior longitudinal fasciculus in the human brain. Brain Struct. Funct. 221, 2075–2092. doi:10.1007/s00429-015-1028-5.

Westerhausen, R., Huster, R.J., Kreuder, F., Wittling, W., Schweiger, E., 2007. Corticospinal tract asymmetries at the level of the internal capsule: is there an association with handedness? Neuroimage 37, 379–386. doi:10.1016/j.neuroimage.2007.05.047.

Winkler, A.M., Ridgway, G.R., Webster, M.A., Smith, S.M., Nichols, T.E., 2014. Permutation inference for the general linear model. Neuroimage 92, 381–397. doi:10.1016/j.neuroimage.2014.01.060.

Wu, Y., Sun, D., Wang, Yong, Wang, Yibao, 2016. Subcomponents and connectivity of the inferior fronto-occipital fasciculus revealed by diffusion spectrum imaging fiber tracking. Front. Neuroanat. 10, 88. doi:10.3389/fnana.2016.00088.

Yogarajah, M., Focke, N.K., Bonelli, S., Cercignani, M., Acheson, J., Parker, G.J.M., Alexander, D.C., McEvoy, A.W., Symms, M.R., Koepp, M.J., Duncan, J.S., 2009. Defining Meyer's loop–temporal lobe resections, visual field deficits and diffusion tensor tractography. Brain 132, 1656–1668. doi:10.1093/brain/awp114.